Dielectric Constant, Metallization Criterion and Optical Properties of CuO Doped TeO_2-B_2O_3 Glasses

NAZIRUL NAZRIN SHAHROL NIDZAM (nazirulnazrin@ymail.com)
University Putra Malaysia

S.A. Umar
Federal University of Lafia

M.K. Halimah
University Putra Malaysia

M.M. Marian
University Putra Malaysia

Z.W. Najwa
University Putra Malaysia

M.S. Jufa
University Putra Malaysia

M.T. Syahirah
University Putra Malaysia

Z. Zuhasanah
University Putra Malaysia

M.N. Azlan
Universiti Pendidikan Sultan Idris

I.G. Geidam
University Putra Malaysia

Imed Boukhris
King Khalid University

Research Article

Keywords: Optical Properties, Refractive Index, Metallization Criterion, Dielectric Constant, Divalent Copper Oxide

Posted Date: December 20th, 2021

DOI: https://doi.org/10.21203/rs.3.rs-1175617/v1

Abstract

Copper oxide doped TeO_2 – B_2O_3 glass system with empirical formula; $[(B_2O_3)_{0.3}(TeO_2)_{0.7}]_{1-x}(CuO)_x$ using the melt quenching method, where x = 0.0, 0.01, 0.015, 0.02, and 0.025 was combined. The glass samples' density and molar volume were measured, followed by characterizations using the UV-Vis, Fourier transform infrared (FTIR) and X-ray diffraction (XRD) spectroscopes. The amorphous or glassy nature of glass samples was proven by the XRD spectra except for the pure borotellurite sample which showed a peak around $2\theta = 20^o$, indicating α-TeO_2 crystalline phase presence. The FTIR spectral analysis suggested the presence of BO_3, TeO_3 and TeO_4 as the structural functional units in the glass samples. The UV-Vis spectra showed no presence of any sharply defined edges, affirming the amorphous or glassy nature of the glass materials. Physical parameters e.g. molar volume, density, oxygen packing density (OPD), inter ionic distance of Cu^{2+} ions, concentration of copper ion per unit volume (N), as well as the polaron radius data were presented and discussed. Also, the direct bandgap (3.8900 to 3.5900 eV) , indirect bandgap (3.3200 to 3.0800 eV), refractive index (2.318 to 2.378), dielectric constant (5.3731 to 5.6549), optical dielectric constant (4.3731 to 4.6549), refractive index based metallization criterion (0.406885 to 0.391916) and the band gap based metallization criterion (0.407431 to 0.392428) were analysed and discussed. Based on the metallization criterion and values of refractive index, the glasses are good candidates for optoelectronic and laser applications. Meanwhile, the dielectric constants' values of the present glasses indicate their suitability bandpass filters and microelectronic substrates applications.

1.0 Introduction

Research studies on various glass compositions have been on the raise over the recent decades with focus on various applications of interest in different fields of technology[1][2]. Technologists and scientists in the glass industry have been considering tellurium oxide for fabrication of different compositions of glasses to satisfy different application interests [3]. This is because TeO_2 offer multitude of advantages over other known glass forming oxides (SiO_2, B_2O_3, P_2O_5, and GeO_2), which include interesting physical properties, high refractive index, non-hygroscopic nature, great transmission of infrared in a wide range of wavelength, high Stark splitting effect, high rare earth ions solubility, low phonon energy as well as low crystallization ability [4][5]. According to Chen et al. (2015) [6], Azlan et al. (2019) [7] and Umar et al. (2017)[8], tellurite glasses offer poor thermal and chemical stabilities as well as high phonon energies which require the addition of other oxides such as SiO_2 [9], B_2O_3 [10], P_2O_5 [6], ZnO [11] and other modifier oxides for improvements.

Boron oxide is one of the most effective of all the oxide glass formers in terms of ease of fabrication [12]. Borate glasses possess low melting temperature, high ability for glass formation, high optical clarity, great radiation and thermal stability, as well as great capacity in-terms of their solubility to transition metals or rare earth ions [13][14]. The quantum efficiency of emissions from rare earth ions (doped) is reduced because of the high phonon energies of the borate glasses [14].

Copper oxide is a transition metal oxide (TMO) that exhibits semiconducting properties The addition of copper in glasses improves the their quality by enhancing the IR transmission and the structural features [15][16]. Copper in glasses exist in three different states, which includes monovalent copper ion (Cu^{+}), divalent copper ion (Cu^{2+}) and metallic copper (Cu), with different coordination geometry and electronic structure [16][17]. Marzouk (2009) [18] had reported in his study, that the addition of copper oxide changed the numerical value of network bonds per unit volume in the studied glass system. Also, having small ionic radius; the Cu ions were suitable in the glass network thereby, creating a cross-linkage between structural units and thus improves the stability of the glass.

This work tried to synthesis a system of divalent CuO doped TeO_2 – B_2O_3 glasses with the objective of studying their dielectric constants, metallization criterion and optical properties. In addition, some physical and structural parameters which include density, polaron radius, oxygen packing density, field strength of Cu^{2+} ions, XRD and FTIR spectra were studied for the fabricated glasses.

2.0 Experimental Section

This section presents the material and methods adopted in carrying out this study. It contains the glass fabrication subsection and the characterization subsection.

2.1 Glass Fabrication

Borotellurite glass system doped with CuO was fabricated using powdered boron oxide (B_2O_3), tellurium oxide (TeO_2) and copper oxide (CuO) as starting materials. Specific amounts of B_2O_3, TeO_2 and CuO were determined with an electronic balance (digital) based on their proportion in the empirical formula $[\left(B_2O_3\right)_{0.3}\left(TeO_2\right)_{0.7}]_{1-x}(CuO)_x$ and about 10 g (total mass) was mixed alumina crucible for each glass sample as presented in Table 1.

Table 1
The molecular weight of each chemical composition of the glass system with respect to different concentration of dopants

Molar fraction x (mol)	B_2O_3 (g)	TeO_2 (g)	CuO (g)	Total (g)
0.000	1.575	8.425	0.000	10
0.005	1.570	8.400	0.030	10
0.010	1.566	8.374	0.060	10
0.015	1.561	8.349	0.091	10
0.020	1.556	8.323	0.121	10

Within the thirty (30) minutes period, the chemical mixture was vigorously stirred to achieve mixture uniformity. At 400°C for one hour, the homogeneous mixture in the alumina crucible was heated in an

electric furnace to eliminate any moisture due to the hygroscopic nature of B_2O_3 [10]. Again at 900°C for melting, the crucible was then heated for two hours. The molten material was turned into a preheated (at 400 ^oC) stainless steel mould cylindrically and then transferred back to the furnace set at 400 ^oC for annealing (for two hour). The furnace (with the solidified glass sample) was later switched-off to cool to a room temperature.

The fabricated samples were cut to an average thickness 2 mm, then polished to give parallel and shiny surfaces for UV-Vis spectroscopy. A portion of each sample prepared, crushed into powdered form for FTIR and XRD characterizations.

2.2 Characterizations and Measurements

Measurements of density was carried out with an electronic-enabled densimeter (Model: MD-300S Alfa mirage) with precision, ±0.001 g/cm^3. The working principle of the device is based the Archimedes with water as liquid of immersion. From the samples' density and molar mass, its molar volume was calculated. The data collection of the XRD was performed at $20^o \leq 2\theta \leq 80^o$ at a step of 0.01^o with the aid of an X-ray diffractometer (Model: PANalytical X'Pert PRO PW3050/60) attached to a control unit (i.e. Programmable). The collection and recording of the data for FTIR spectra was performed under the ambient condition using the 1650 PerkinElmer FTIR Spectrometer model. A system of UV - 1650PC Shidamatsu Model of UV - Vis spectrometer was utilized for the absorbance data collection for the glass samples over the wavelength range of 200 to 800 nm.

3.0 Result And Discussion

Figure 1 deduces the different variety in composition of $TeO_2 - B_2O_3$ doped CuO glasses through XRD pattern. With the exception of sample 0.00 mol% of CuO which shows a peak around the position $25^\circ < 2\theta < 30^o$, all the samples presented no sharp peak but a broad hump can be seen at the position of 2θ within 20° to 30°. According to Baizura and Yahya (2011) [19] and Umar et al. (2018)[9], the crystalline peak displayed represents the presence of $\propto -\mathrm{TeO}_2$ or $\gamma - \mathrm{TeO}_2$ crystalline phase in the sample. Besides that, the formation of the crystalline phase might be due to the duration of the melting process during the synthesis of the glass sample. Rosmawati *et al*., (2008) [20] suggested that the broad hump observed represents short range of regularly arranged of atoms indicating the glassy phase (amorphous nature).

FTIR spectroscopy as tool is useful for studying the functional groups that are fundamental to crystalline and non-crystalline materials [10][21]. Figure 2 shows the infra-red (IR) spectra of copper oxide doped borotellurite glasses in the wavenumber range of 280 to 1800 cm^{-1}. Table 2 displays the assignments of the infrared transmission bands for the studied glasses. The IR spectral absorption from borate glasses can be classified into two: The B - O stretching for the units of tetrahedral BO_4 occurs between 800 and 1200 cm^{-1}, while the B - O stretching of trigonal BO_3 units occurs between 1200 and 1800 cm^{-1} [9]. The stretching vibrations of trigonal B - O bond in BO_3 units from boroxyl groups is represented by the

absorption band located around 1226 – 1234 cm^{-1} and 1381 – 1367 cm^{-1}[1][3]. Halimah et al.[22], recorded the absorption band around 1381 – 1367 cm^{-1} is for a BO_3 structure with one NBO and two BOs, while the 1226 – 1234 cm^{-1} band comes from the BO_3 units with three BOs surrounding the boron atom.

According to Hajer et al. [23], the trigonal (TeO_4) based Te - O bonds, and trigonal pyramid (TeO_3) whose stretching vibrations were assigned to the absorption bands from 600 and 700 cm^{-1}. The stretching vibrations of Te – O in TeO_3 groups are with higher frequency compared with the TeO_4 groups. The TeO_4 (trigonal bipyramid) forms the first band around 600–650 cm^{-1}, while the TeO_3, trigonal pyramid forms the second band around 650 – 700 cm^{-1} [24].

According to Muhammad Noorazlan et al, (2013) [25], the low concentration of the element itself that could not be detected by the instrument led to the vanished absorption spectra. This fact might have resulted to the absence of Cu-O absorption band in the present glasses.

Table 2
IR absorption bands of CuO Doped Borotellurite Glass System

No.	0.000	0.005	0.010	0.015	0.020	Assignments
1	-	660-680	660-680	660-680	660-680	TeO stretching vibrations in TeO_3 [12]
2	-	541	544	533	548	Te-O vibrations in TeO_4 units
3	1226.46	1232.16	1232.33	1234.67	1234.02	B-O stretching vibration of BO_3 units [9]
4	1381.89	1369.54	1367.65	1366.65	1367.86	B-O stretching vibration ofBO_3 [12]
5	1637.65	-	-	-	-	Isolated pyro-borate group based B-O^- bond [13]

The glass density for each sample was evaluated in accordance with the famous Archimedes' principle by using the following formula as reported in [26]:

$$\rho_{sample} = {}^{w_{air}}/_{w_{water}} x\, \rho_{water} \quad (1)$$

where ρ_{sample} is the gl ass sample's density, ρ_{water} is the water density (1 g/cm^3), w_{water} is immersed sample's weight in the distilled water and w_{air} is the sample's weight in air.

The value of molar volume can be obtained right after the result of density was measured by using the following formula as reported by Abdulbaset et al [26]:

$$V_m = \frac{M_w}{\rho_{sample}}$$

2

where ρ = sample's density in g/$cm^3$and M_w = glass molecular weight in g/mol.

Table 3
Density and Molar volume of Borotellurite Glass System Doped with various concentration of Copper Oxide

Molar Fraction x (mol)	Density (g/cm^3)	Molar Volume (cm^3/mol)
0.000	4.373	30.327
0.005	4.100	32.436
0.010	3.710	35.966
0.015	3.644	36.714
0.020	3.504	38.296

Based on tabulated data in Table 3 and Figure 3, the borotellurite glass system doped with copper oxide has its density decreased from 4.373 to 3.504 g/cm^3 as the CuO concentration increases because of the CuO introduction into the glass network breaks bonds and creates more non-bridging oxygen. The presence of dopant breaks up the Te-O-Te linkage and increases the free space in glass structure and therefore more non-bridging oxygen (NBO) starts to form [27]. The presence of NBO makes the glass network less compact and increase the fragility as well [28].

Besides that, the decrease in the glass density can be attributed to the substitution heavier atoms of Te (229.2 g/mol) with lighter Cu (79.55 g/mol) atoms [11][22].

Increase in molar concentration of CuO in Figure 3 as shown results to the corresponding increase in the glasses' molar volume from 30.3269 to 38.2955 cm^3/mol. This can be related to the rise in the formation of more single bonded oxygen atoms which creates a wider inter-atomic spacing between the glass system's networked atoms. Thus, more interstices between the atoms are created with the introduction of more Cu^{2+} ions in the network structure [24][29]. According to Eevon et al., (2016) [15], the formation of more open spaces and excess free volume in the network of the glass is gotten from the more non-bridging oxygen creation. Therefore, the process lead to a drop in the rigidity and glass network's strength.

Figure 4 presents the optical absorbance spectra obtained from the UV-Vis spectroscopy performed at room temperature for TeO_2 – B_2O_3 doped CuO glasses over 200 to 800 nm of the wavelength range. To study optical absorption spectra, especially the absorption edge is an important method employed for studying induced transitions optically and further acquiring the knowledge about the band structure and energy gap of both non-crystalline and crystalline materials [13]. The absence of sharp absorption edges

in the spectral figure confirms the amorphous or glassy nature of the glasses as earlier suggested by the XRD results [14][25]. Naturally, the position of the absorption edge is simply defined by the strength of the oxygen bond in the network formation of the glass [23][30]. The characteristic absorption edge is influenced by changes in oxygen bonding within the glass network [9]. The absorption edge changes to a higher wavelength as the CuO concentration tend to increases. The formation of non-bridging oxygen (NBO) which bonded to the network by a single bond is responsible for the absorption edge shift to longer wavelength range [31].

In order to quantify the indirect and direct transitions that occur in a band gap, Mott and Davis suggested a relationship between the photon energy and absorption coefficient. The expression is given in this relation:

$$\alpha(\omega) = B\frac{(\hbar\omega - E_{opt})^n}{\hbar\omega}$$

3

where n=1/2 for direct transition and n = 2 for indirect transition, B is a constant related to the extent of the band tailing, E_{opt} is the optical energy gap between the ground state and the energized state, $\alpha(\omega)$ is the absorption coefficient at an angular frequency of ω=2πf and ħω is the photon energy [42]. Electromagnetic waves interfere with the electron in the ground state in both cases, causing it to rise through the fundamental distance to the energised state [7][14]. Using the relation below, the optical absorption coefficient α (v) was computed for each sample by:

$$\alpha(\omega) = 2.303\frac{A}{t}$$

4

where t denotes the glass thickness and A denotes the absorbance of the glass sample respectively.

The energies of optical band gap (E_{opt}) are evaluated through extrapolation of the linear parts of $(\alpha\hbar\omega)^2$ and $(\alpha\hbar\omega)^{1/2}$ curves against ħω.

For direct transition:

$$(\alpha\hbar\omega)^2 = B(\hbar\omega - E_{opt})$$

5

whereas for indirect transition

$$(\alpha\hbar\omega)^{1/2} = B(\hbar\omega - E_{opt})$$

6

The refractive index, n is the measure of a material compactness [9]. Material's refractive index is influenced mostly by its density, electronic polarizability, molecular orientation, photo refractive effects and thermal effects among others [3].

Using the optical band gap data as reported by Halimah et al. [10], it can computed as follows;

$$\frac{n^2-1}{n^2+2} = 1 - \sqrt{\frac{E_g}{20}}$$

7

where, E_{opt} the energy of optical band gap and n is is the index of refraction.

The molar refraction (R_m) was calculated by using the relation:

$$R_m = \left(\frac{n^2-1}{n^2+2}\right) V_m$$

8

where $V_m =$ the molecular volume and n = the refractive index.

Figure 5 and 6 demonstrates the extrapolation of plots of $(\alpha\square\square)^2$ and $(\alpha\square\square)^{1/2}$ versus energy of the photon ($\square\square$) respectively used for direct and indirect optical band gap energies evaluation. Table 4 shows the values of the band gap energies obtained for both direct and indirect transitions which are plotted against the molar fraction of CuO as shown in Figure 7. The CuO molar fraction gradually increased from 0.000 to 0.020 mol, the direct energy band gap decreased from 3.89 to 3.59 eV, whereas the indirect energy band gap decreased from 3.32 to 3.08 eV. Such phenomenon is mostly expected when the addition of dopant results in the breakage of bonds connecting some oxygen atoms with double bonds and leaving them with single bond connections to the structure of the glass network giving rise to the formation of what is commonly known as non-bridging oxygen. which causes a randomised glass structure [5][27]. The inclusion of CuO causes the regular structure of the borotellurite glass system to deform and eventually break [29]. The band gap's decrement can also be linked to an increased number of disordered atoms. Consequently, this lead to more add-on of the localized states within the gap [13][32]. Rao et al., (2012)[33] mentioned that reduction in optical energy band gap (E_{opt}) specifies formation of more non-bridging oxygen atoms (NBO).

Table 4

Direct Energy Band Gap, E^1_{opt}, Indirect Energy Band Gap, E^2_{opt} and Urbach Energy, ΔE of Borotellurite Glasses System Doped with Copper Oxide

Molar fraction, x	Direct Energy Band Gap, E^1_{opt} (±0.0630 eV)	Indirect Energy Band Gap, E^2_{opt} (±0.0445 eV)	Urbach Energy, ΔE (±0.0481 eV)
0.000	3.89	3.32	1.185
0.005	3.87	3.30	1.157
0.010	3.68	3.21	1.429
0.015	3.62	3.16	1.225
0.020	3.59	3.08	1.220

The details on the degree of the disorder of the atoms in the materials (amorphous and crystalline) is given by the Urbach energy, ΔE [8][34]. According to Noorazlan et al.[35], temperature, static disorder, mediated disorder, heavy ionic bonds, as well as average phonon energies influence Urbach force. A plot of the natural logarithm of the absorption coefficient (α) as a function of photon energy ($\hbar\omega$) can be used to calculate its slope, which is given by [36]:

$$\alpha(\omega) = \beta \exp\left(\frac{\hbar\omega}{\Delta E}\right) \quad (9)$$

where $\hbar$ is the plank constant, β is a constant, and ΔE is the Urbach energy which specifies the width of the band tails of the localized state [34]. As shown in Figure 8, by taking the reciprocals of the slopes of the portion in the lower photon energy curves, the values of Urbach energy are calculated [37].

Table 5 shows the tabulated data of Urbach energy obtained and a graph of Urbach energy versus the molar fraction of CuO was plotted as shown in Figure 9. The Urbach energy, which is related to the scale of disorderliness in the network of the glass, is reduced when more concentration of CuO is added to the glass system [38]. This corresponds to the reduction in the non-bridging oxygen's number in the glass network. The creation of more defects as well as an increasing number of single bonded oxygen atoms in the network of the glass can be associated with the Urbach energy increment. Therefore, the phonons tend to collide more frequently which consequently reduces atomic mobility in the network. When a material has a high Urbach force, it is more likely to transform weak bonds into defects. To put it another way, a high Urbach energy means that there are more flaws in a glass network [3][39].

Figure 10 and Table 5 shows the molar refractive index and the refractive index of the copper oxide doped borotellurite glasses system. The refractive index is determined using equation (7) substitution the value of the band gap energy (E_{opt}) and solving for n [24], [29]. The value increased from 2.318 to 2.378 as the molar fraction of CuO increases from 0.000 to 0.020 mol. The refractive index is a basic property of glass that can be used to assess its suitability for applications in optical technologies [30]. The increased value

of the refractive index might be explained as due to the increase in the polarizability of first neighbour ions coordinated with anion, the coordination number of the ion, electrical polarizability of the oxide ion, and optical basicity of the glasses resulting from the increase in electron mobility [4], [25].

The molar refractive index is determined from the refractive index value as presented in equation 8. The studied glasses R_m value increased from 17.9874 to 23.2872 with percentage rise in the concentration of CuO from 0 to 2%. The molar refractive index is dependent on the electron mobility which is increased with additional bond breakage creating more non-bridging oxygen which increases polarizability [13].

Table 5
Index of Refraction (n), Molar Refraction (Rm) and Oxygen Packing Density (OPD) of Borotellurite Glasses Doped with Copper oxide,$[(B_2O_3)_{0.3}\left(TeO_2\right)_{0.7}]_{1-x}(CuO)_x$

X	n (±0.01125)	R_m (±0.97045)	OPD(±2.822 cm^{-3})
0.000	2.318	17.9874	75.84831
0.005	2.321	19.2634	71.0544
0.010	2.345	21.5774	64.24213
0.015	2.357	22.1363	63.04658
0.020	2.378	23.2872	60.5735

The variation of refractive index based metallization criterion and oxygen packing density (OPD) against the molar fraction of CuO in TeO_2 – B_2O_3 doped CuO glass system is presented in Figure 11. The value as presented in Table 5 and Figure 11 decreased from 75.84831 to 60.5735 cm^{-3} with rise in concentration of CuO from 0 to 2%. The OPD evaluates the level tightness with which the oxygen atoms are packed and is used in examining the structural formative changes observed in the network of the glass system [40]. The decrease in the OPD with increase CuO concentration indicates the creation of more interstitial spacing between the constituting atoms which might have resulted from the formation of more double bonded oxygen atoms [41].

The refractive index based metallization criterion (M_n) values which decreased from 0.406885to 0.391916 with slow increase in the Copper Oxide concentration from 0 to 2% are presented in Table 6. The metallization criterion drop is a very clear indication of the broadening of both the valence and conduction bands resulting to the shrinkage of the band gap [5].

The refractive index based metallization criterion (M_n) is obtained from the molar refractivity (R_m) and molar volume (V_m) as proposed in the Lorentz–Lorenz equation [42];

$$M = 1 - {}^{R_m}/_{V_m} \quad 10$$

The band gap based metallization criterion (M_{E_g}) is calculated by substituting $R_m = V_m\left(1 - \sqrt{\frac{E_g}{20}}\right)$ (with$E_g =$ the indirect band gap energy of glass sample) as reported by Kundu et al.[41] in to equation (11) to get;

M=\sqrt{\frac{{E}_{g}}{20}}

11

Herzfeld's theory of condensed matter metallization explained that as the refractive index approaches infinity (i.e n\to \infty), $R_m/V_m \to 1$ as presented in the Lorentz-Lorenz equation, i.e. follows the metallization in the solid covalent materials [43]. In this situation, the material acquires the status of a metal when electrons get freedom of movements within the material [41][42]. According to Dimitrov and Komatsu (2005) [42], at the transition point between metallic and non-metallic phases, the metallization criterion is zero. Umar et al. (2017)[8] reported that glasses with metallization criterion possess good optical nonlinearity in the value range of between 0.3 to 0.45 and thus present promising potential in laser and non-linear optical applications.

Table 6
Oxygen Packing Density (OPD), Metallization Criterion, Coefficient of Transmission and Reflection Loss, Dielectric Constant and Optical Dielectric Constant of Borotellurite Glasses System Doped with Copper Oxide

X	{M}_{{E}_{g}} (±0.0028)	{M}_{n} (±0.0028)	T (±0.0024)	{R}_{L} (±0.0016)	\epsilon (±0.053)	{\epsilon }_{opt} (±0.053)
0	0.407431	0.406885	0.72743	0.157789	5.373124	4.373124
0.005	0.406202	0.40611	0.726784	0.158222	5.387041	4.387041
0.01	0.400625	0.400061	0.721647	0.161679	5.499025	4.499025
0.015	0.397492	0.397061	0.719096	0.163402	5.555449	4.555449
0.02	0.392428	0.391916	0.714663	0.16641	5.654884	4.654884

Figure 12 presents the variation in the transmission coefficient and reflection loss values against the molar concentration of CuO in CuO doped borotellurite glass system. The transmission coefficient values decreased from 0.7274 to 0.7147 while the reflection loss increased from 0.1578 to 0.1664 with increasing concentration of CuO from 0 to 2%. The optical transmission coefficient and the reflection loss values represent the fraction of incident wave transmitted and reflected respectively. The inverse relationship between the two parameters confirmed the theoretical submission of reciprocity characterizing them [8], [44]. The values of the coefficient of transmission and Reflection loss are determined from the value of the refractive index by using the Fresnel's formula as stated by Umar et al. (2019) [29] and Ali et al. (2019) [44];

{{ R}_{L}=\left(\frac{n-1}{n+1}\right)}^{2}
12
T=\frac{2n}{{n}^{2}+1}
13
Table 7 present the values of the Cu^{2+} ion concentration, Inter-nuclear distance of Cu^{2+} ions, polaron radius and field strength of CU^{2+} ions yield for CuO doped borotellurite glasses. The ion concentration of Cu^{2+} increased from 0 to 3.2082 x 10^{20} ions/ cm^3 as the CuO molar concentration in the studied glasses was increased from 0 to 2%. The Cu^{2+} ions concentration was computed using the equation (14) as reported by [45].

Table 7
Ion concentration of Cu^{2+} ions (N), Inter-nuclear distance of Cu^{2+} ions (R_i), Polaron Radius (R_p) and Field Strength of CU^{2+} ions Yield (F)

x	N (E+20 cm^{-3})	{R}_{i} (Å)	{R}_{p} (Å)	F (E+15 cm^{-2})
0	0	-	-	-
0.005	0.93283	11.02475692	8.886431753	3.672342494
0.01	1.691588	9.040764823	7.287249603	5.460981527
0.015	2.497258	7.939908802	6.399912607	7.080271488
0.02	3.208211	7.303802488	5.88718368	8.367251555

N = \frac{{X}_{Cu}x \rho x{N}_{A}}{{m}_{w}} (14)

where ρ, {N}_{A}, {X}_{Cu} and {M}_{w} are the glass density, Avogadro's number, molar fraction and the glass molar weight of CuO in the glass sample respectively.

The inter-nuclear distance of Cu^{2+} ions, the polaron radius and the field strength of CU^{2+} ions yield are determined using the formula as reported in [29], [45], [46];

{R}_{i} = {\left(\frac{1}{N}\right)}^{1/3}
15
{R}_{p}= \frac{1}{2}{\left(\frac{\pi }{6N}\right)}^{1/3}
16
F = \frac{Z}{{R}_{p}^{2}} (17)

The values of both dielectric constant and optical dielectric constant inclusive of the variation with CuO molar concentration are presented in Table 6 and Figure 13 respectively. Dielectric behaviours in materials are results of extrinsic and intrinsic factors such as oxygen vacancies, porosity, grain size, lattice vibration modes as well as chemical homogeneity [47]. According to Zulkefly et al. (2016) [48], the

dielectric features at lower frequencies depend on the ionic, electronic interfacial and dipolar polarizations and thus alternating voltage induces the diffusion of mobile charges usually impurity ions.

The dielectric constant and the optical dielectric constant are expressed as functions of refractive index (n) as reported by [44][45] in equations (18) and (19) respectively;

\epsilon ={n}^{2}
18
{\epsilon }_{opt}=p\frac{dt}{dp}={n}^{2}-1
19
The increased values of the dielectric and optical dielectric constants from 5.373124 to 5.654884 and 4.373124 to 4.654885 with increased concentration in the dopant (CuO) from 0 to 2% respectively as shown in Table 6 and Figure 13 respectively. Increase in dielectric constant is usually a result of increased polarizability from the electronic and ionic contributions. This might be coming from either bond breakage which results to formation of more free and polarizable oxygen atoms or the substitution of lower cation polarizable atoms with higher ones or both. In the case of the present glasses, the density, molar volume as well as the FTIR results suggested that more oxygen atoms are freed through bond breakage and formation of more single bonded oxygen atoms which enhances the overall electronic and ion polarizability in the glass system [48]. Also, substitution of B^{3+} ions (0.002 $Å^3$) with more polarizable ions of Cu^{2+} (1.2 $Å^3$) might have led to an improved ion polarizability which improves the dielectric constant [49][50]. According to Varshneya et al. (2019) [51], Umar et al. (2021)[4] and Asma'u (2015)[52], glasses and glass-ceramics with dielectric constant in the range of the values obtained for the present glasses can be used in the fabrication of microelectronic substrates and packaging materials.

Conclusion

A copper oxide doped borotellurite glass system series with a chemical formula {[\left({{\text{B}}_{2}{\text{O}}_{3}){}_{0.3}{\left(\text{T}\text{e}{\text{O}}_{2}\right)}_{0.7}\right]}_{1-x}{\left(\text{C}\text{u}\text{O}\right)}_{x} where, melt quenching method was used to synthesize x = 0, 0.005, 0.010, 0.015 and 0.020. The density as well as molar volume were measured, while the XRD, FTIR and UVU-Vis characterizations were used for the study of physical, structural, dielectric constant, metallization criterion and optical properties of the glasses. With the exception of the x = 0.0 mol sample which shows a crystalline phase reprinting alpha and beta TeO_2 phase, all the samples showed no sharp peaks and represented no crystalline phase but glassy materials. FTIR analysis indicated the presence of TeO_3, TeO_4, {\text{B}\text{O}}_{3} and BO_2O and B-{\text{O}}^{-}bond in isolated pyroborate group in glass samples. The density of glasses decreased while the molar volume increased with CuO concentration. Refractive index, molar refraction, UV-Vis absorption spectra, transmission coefficient, polaron radius, oxygen packing density, refractive index and band gap based metallization criterion, relative permittivity (i.e. optical dielectric constant and dielectric constant) were all studied. The absorption spectra show the absence of sharp absorption edges which indicate the characteristics of the glassy material. Moreover, the indirect and direct energy band gap decreased from 3.32 to 3.08 eV and 3.89 to 3.59 eV respectively

as the CuO concentration increases. The refractive index jumps from 2.318 to 2.378 resulting from the non-bridging oxygen (NBO) atoms' production with more polarizability than bridging oxygen. The refractive index and Band gap based metallization criterion increased from 0.406885 to 0.391916 and 0.407431 to 0.392428 respectively. While the values of the dielectric and optical dielectric constants increased from 5.3731 to 5.6548 and 4.3731 to 4.6548 respectively with increase in the dopant (CuO) concentration. The values of the refractive index, metallization criterion, and the dielectric constants fall in the category of glasses with great potentials for application in optical filters, nonlinear optical applications (lasers, optical switches etc.), microelectronic substrates and packaging materials.

Declarations

The authors declare that they have no known competing financial interests or personal relationships that could have appeared to influence the work reported in this paper.

Acknowledgement

The authors extend their appreciation to the Deanship of Scientific Research at King Khalid University, Saudi Arabia for funding this work through Research Groups Program under grant number R.G.P.2/187/42.

References

1. M.N. Azlan, M.K. Halimah, S.S. Hajer, A.B. Suraini, Y. Azlina, S.A. Umar, Enhanced Optical Performance of Tellurite Glass Doped with Samarium Nanoparticles for Fiber Optics Application. Chalcogenide Lett. **16**(5), 215–229 (2019). doi:10.1016/j.jnoncrysol.2017.07.013
2. H.R. Shaari et al., "Investigation of Structural and Optical Properties of Graphene Oxide – Coated Neodymium Nanoparticles Doped Zinc – Tellurite Glass for Glass Fiber," J. Inorg. Organomet. Polym Mater., 1–11, 2021, doi:10.1007/s10904-021-02061-7
3. M.N. Azlan et al., Linear and Nonlinear Optical Efficiency of Novel Neodymium Nanoparticles Doped Tellurite Glass for Advanced Laser Glass. Educ. JSMT **5**(2), 47–66 (2018)
4. S.A. Umar et al., Oxide ion / electronic polarizability, optical basicity and linear dielectric susceptibility of TeO 2 – B 2 O 3 – SiO 2 glasses. Ceram. Int. **47**(15), 21668–21678 (2021). doi:10.1016/j.ceramint.2021.04.180
5. Y. Azlina, M.N. Azlan, M.K. Halimah, S.A. Umar, R. El-mallawany, G. Najmi, "Optical performance of neodymium nanoparticles doped tellurite glasses," *Phys. B Phys. Condens. Matter*, vol. 577, no. October 2019, p. 411784, 2020, doi: 10.1016/j.physb.2019.411784
6. R. Chen et al., 2 μm fluorescence of Ho3+:5I7→5I8transition sensitized by Er3+in tellurite germanate glasses. Opt. Mater. (Amst). **49**, 116–122 (2015). doi:10.1016/j.optmat.2015.09.003
7. M.N. Azlan, M.K. Halimah, A.B. Suriani, Y. Azlina, S.A. Umar, R. El-mallawany, "Upconversion properties of erbium nanoparticles doped tellurite glasses for high efficient laser glass," *Opt.*

Commun., vol. 448, no. April, pp. 82–88, 2019, doi: 10.1016/j.optcom.2019.05.022

8. S.A.A. Umar, M.K.K. Halimah, K.T.T. Chan, A.A.A. Latif, "Physical, structural and optical properties of erbium doped rice husk silicate borotellurite (Er-doped RHSBT) glasses," *J. Non. Cryst. Solids*, vol. 472, no. July, pp. 31–38, 2017, doi: 10.1016/j.jnoncrysol.2017.07.013
9. S.A. Umar, M.K. Halimah, A.M. Hamza, A.A. Abdulbaset, "The Structural, Physical and Optical Properties of Borotellurite Glasses Incorporated with Silica from Rice Husk," *J. Sci. Math. Lett.*, vol. 6, no. 2018, pp. 32–46, 2018
10. M.K. Halimah et al., "Effect of erbium nanoparticles on structural and spectroscopic properties of bio-silica borotellurite glasses containing silver oxide," Mater. Chem. Phys., 236, no. June, 121795, 2019, doi:10.1016/j.matchemphys.2019.121795
11. S.H.S.H. Alazoumi et al., "Optical properties of zinc lead tellurite glasses," *Results Phys.*, vol. 9, no. March, pp. 1371–1376, 2018, doi: 10.1016/j.rinp.2018.04.041
12. A. Kaur, A. Khanna, F. González, C. Pesquera, B. Chen, Structural, optical, dielectric and thermal properties of molybdenum tellurite and borotellurite glasses. J. Non. Cryst. Solids **444**, 1–10 (2016). doi:10.1016/j.jnoncrysol.2016.04.033
13. S.A. Umar et al., Spectroscopic investigations of Er2O3 doped silica borotellurite glasses. Opt. Mater. (Amst). **114**, no. March, p. 110987 (2021). doi:10.1016/j.optmat.2021.110987
14. G. Lakshminarayana et al., Physical, structural, thermal, and optical spectroscopy studies of TeO2–B2O3–MoO3–ZnO–R2O (R = Li, Na, and K)/MO (M = Mg, Ca, and Pb) glasses. J. Alloys Compd. **690**, 799–816 (2017). doi:10.1016/j.jallcom.2016.08.180
15. N. Kaur, A. Khanna, P.S.R. Krishna, F. González, "Optical properties of borotellurite glasses containing metal oxides," in *AIP Conference Proceedings*, 2015, vol. 1665, p. 070029, doi: 10.1063/1.4917893
16. M. Attallah, M. Farouk, A. El-Korashy, M. ElOkr, Copper Doped Phosphate Glass as an Optical Bandpass Filter. Silicon **10**(2), 547–554 (2018). doi:10.1007/s12633-016-9488-7
17. A. Samir, M.A. Hassan, A. Abokhadra, L.I. Soliman, M. Elokr, Characterization of borate glasses doped with copper oxide for optical application. Opt. Quantum Electron. **51**(4), 1–13 (2019). doi:10.1007/s11082-019-1819-7
18. S.Y. Marzouk, Ultrasonic and infrared measurements of copper-doped sodium phosphate glasses. Mater. Chem. Phys. **114**(1), 188–193 (2009). doi:10.1016/j.matchemphys.2008.09.021
19. N. Baizura, A.K. Yahya, Effects of Nb2O5 Replacement by Er2O 3 on elastic and structural properties of 75TeO2-(10 - X)Nb2O5-15ZnO-(x)Er2O3 glass. J. Non. Cryst. Solids **357**(15), 2810–2815 (2011). doi:10.1016/j.jnoncrysol.2011.03.003
20. S. Rosmawati, H.A.A. Sidek, A.T. Zainal, H. Mohd Zobir, Effect of Zinc on the Physical Properties of Tellurite Glass. J. Appl. Sci. **8**(10), 1956–1961 (2013). doi:10.3923/jas.2008.1956.1961
21. S.A. Umar et al., Structural, elastic and thermo – physical properties of Er 2 O 3 nanoparticles doped bio – silicate borotellurite glasses. SN Appl. Sci. **291**, 1–10 (2020). doi:10.1007/s42452-020-2112-x

22. M.K. Halimah et al., “Study of rice husk silicate effects on the elastic, physical and structural properties of borotellurite glasses,” Mater. Chem. Phys., 238, no. July, 121891, 2019, doi:10.1016/j.matchemphys.2019.121891
23. S.S. Hajer, M.K. Halimah, Z. Azmi, M.N. Azlan, Optical Properties of Zinc-Borotellurite Doped Samarium. Chalcogenide Lett. **11**(11), 553–566 (2014)
24. M.K. Halimah, A.A. Awshah, A.M. Hamza, S.A. Umar, K.T. Chan, S.H. Alazoumi, “Effect of neodymium nanoparticles on optical properties of zinc tellurite glass system,” *J. Mater. Sci. Mater. Electron.*, vol. 31, no. 2020, pp. 3785–3794, 2020, doi: 10.1007/s10854-020-02907-9
25. D.W. Azlan, M.N. Halimah, M.K. Zulkefly, S S and Mohamad, Effect of Erbium Nanoparticles on Optical Properties of Zinc Borotellurite Glass System. J. Nanomater. **8**(2), 49–59 (2013). doi:10.4028/www.scientific.net/MSF.846.63
26. A.A.A. Abdulbaset et al., “Effect of Neodymium Nanoparticles On Elastic Properties Of Zinc Tellurite Glass System,” *Adv. Mater. Sci. Eng.*, vol. 2017, pp. 1–7, 2017
27. R.A. Tafida et al., “Structural, optical and elastic properties of silver oxide incorporated zinc tellurite glass system doped with Sm3+ ions,” Mater. Chem. Phys., 246, no. February, 122801, 2020, doi:10.1016/j.matchemphys.2020.122801
28. S.A. Umar, “Structural, Elastic and Optical Properties of Rice Husk Silicate Borotellurite Glass System Doped with Micro and Nanoparticles of Erbium Oxide,” 2018
29. S.A. Umar et al., “Optical and structural properties of rice husk silicate incorporated borotellurite glasses doped with erbium oxide nanoparticles,” *J. Mater. Sci. Mater. Electron.*, vol. 30, no. 2019, pp. 18606–18616, 2019, doi: 10.1007/s10854-019-02213-z
30. M.F. Fazzny, M.K. Halimah, M.N. Azlan, Effect of Lanthanum Oxide on Optical Properties of Zinc Borotellurite Glass System. J. Optoelectron. Biomed. Mater. **8**(2), 49–59 (2016). doi:10.4028/www.scientific.net/MSF.846.63
31. G. Bilir, A. Kaya, H. Cinkaya, G. Eryürek, “Spectroscopic investigation of zinc tellurite glasses doped with Yb3 +and Er3 +ions,” *Spectrochim. Acta - Part A Mol. Biomol. Spectrosc.*, vol. 165, no. 2016, pp. 183–190, 2016, doi: 10.1016/j.saa.2016.04.042
32. P.P. Pawar, S.R. Munishwar, R.S. Gedam, “Intense white light luminescent Dy3+doped lithium borate glasses for W-LED: A correlation between physical, thermal, structural and optical properties,” *Solid State Sci.*, vol. 64, no. 2017, pp. 41–50, 2017, doi: 10.1016/j.solidstatesciences.2016.12.009
33. G.S. Rao et al., Structural analysis of novel oxyfluoroborate glasses: Correlation between elastic and compositional parameters. Mater. Lett. **68**, 21–23 (2012). doi:10.1016/j.matlet.2011.10.009
34. A. Maaoui, M. Haouari, Z. Zaaboub, I. Fraj, F. Saidi, H. Ben Ouada, “Concentration effects on the optical spectroscopic properties of Er3+- doped TeO2-Nb2O5-ZnO vitreous system,” *J. Alloys Compd.*, vol. 663, no. 2016, pp. 395–406, 2016, doi: 10.1016/j.jallcom.2015.12.130
35. M.N. Azlan, M.K. Halimah, S.Z. Shafinas, W.M. Daud, “Effect of Erbium Nanoparticles on Optical Properties of Zinc Borotellurite Glass System,” *J. Nanomater.* ·, vol. 940917, no. November, p. 8, 2013

36. A. Usman et al., “Influence of Ho3 +ions on structural and optical properties of zinc borotellurite glass system,” *J. Non. Cryst. Solids*, vol. 483, no. December 2017, pp. 18–25, 2018, doi: 10.1016/j.jnoncrysol.2017.12.040
37. C. Eevon, M.K. Halimah, M.N. Azlan, R. El-Mallawany, S.L. Hii, Optical and thermal properties of TeO2-B2O3-Gd2O3 glass systems. Mater. Sci. Pol. (2019). doi:10.2478/msp-2019-0074
38. C. Eevon, M.K. Halimah, A. Zakaria, C.A.C. Azurahanim, M.N. Azlan, M.F. Faznny, Linear and nonlinear optical properties of Gd 3 + doped zinc borotellurite glasses for all-optical switching applications. Results Phys. **6**, 761–766 (2016). doi:10.1016/j.rinp.2016.10.010
39. C.R. Kesavulu et al., Spectroscopic investigations of Nd3+doped gadolinium calcium silica borate glasses for the NIR emission at 1059ï¿½nm. J. Alloys Compd. **695**, 590–598 (2017). doi:10.1016/j.jallcom.2016.11.002
40. H. Guo et al., “Optical band gap and photoluminescence in heavily Tb 3 þ doped GeO 2 -B 2 O 3 -SiO 2 -Ga 2 O 3 magneto-optical glasses,” *J. Alloy. Compd. J.*, vol. 686, no. 2016, pp. 635–640, 2016, doi: 10.1016/j.jallcom.2016.06.074
41. R.S. Kundu, S. Dhankhar, R. Punia, K. Nanda, N. Kishore, Bismuth modified physical, structural and optical properties of mid-IR transparent zinc boro-tellurite glasses. J. Alloys Compd. **587**, 66–73 (2014). doi:10.1016/j.jallcom.2013.10.141
42. V. Dimitrov, T. Komatsu, “Classification of oxide glasses: A polarizability approach,” *J. Solid State Chem.*, vol. 178, no. 2005, pp. 831–846, 2005, doi: 10.1016/j.jssc.2004.12.013
43. B. Bhatia, S.L. Meena, V. Parihar, M. Poonia, “Optical Basicity and Polarizability of Nd 3 + -Doped Bismuth Borate Glasses,” *New J. Glas. Ceram.*, vol. 5, no. July, pp. 44–52, 2015, doi: 10.4236/njgc.2015.53006
44. A.A. Ali, Y.S. Rammah, M.H. Shaaban, “The influence of TiO 2 on structural, physical and optical properties of B 2 O 3 –TeO 2 – Na 2 O – CaO glasses,” *J. Non. Cryst. Solids*, vol. 514, no. February, pp. 52–59, 2019, doi: 10.1016/j.jnoncrysol.2019.03.030
45. K. Annapoorani et al., “Investigations on structural and luminescence behavior of Er3 +doped Lithium Zinc borate glasses for lasers and optical amplifier applications,” *J. Non. Cryst. Solids*, vol. 447, no. 2016, pp. 273–282, 2016, doi: 10.1016/j.jnoncrysol.2016.06.021
46. S.Y. Moustafa, M.R. Sahar, S.K. Ghoshal, Erbium ions oscillator strength and emission enhancement in antimony phosphate amorphous matrix. J. Non. Cryst. Solids **433**, 87–94 (2016). doi:10.1016/j.jnoncrysol.2015.10.038
47. A.I. Borhan, M. Gromada, G.G. Nedelcu, L. Leontie, Influence of additives (CoO, CaO, B 2 O 3) on thermal and dielectric properties of BaO-Al 2 O 3 -SiO 2 glass-ceramic sealant for OTM applications. Ceram. Int. **42**(8), 10459–10468 (2016)
48. S.S. Zulkefly, H.M. Kamari, M.N.A.A. Azis, W.M.D. Wan-Yusoff, “Influence of erbium doping on dielectric properties of zinc borotellurite glass system,” *Mater. Sci. Forum*, vol. 846, no. December 2015, pp. 161–171, 2016, doi: 10.4028/www.scientific.net/MSF.846.161

49. R.R. Reddy, Y.N. Ahammed, P.A. Azeem, K.R. Gopal, T.V.R. Rao, “Electronic Polarizability and Optical Basicity Properties of Oxide Glasses Through Average Electronegativity,” *J. Non. Cryst. Solids*, vol. 286, no. February 2015, pp. 169–180, 2001, doi: 10.1016/S0022-3093(01)00481-1
50. V. Dimitrov, T. Komatsu, Correlation among electronegativity, cation polarizability, optical basicity and single bond strength of simple oxides. J. Solid State Chem. **196**, 574–578 (2012). doi:10.1016/j.jssc.2012.07.030
51. A.K. Varshneya, J.C. Mauro, *Fundamentals of inorganic glass making*. 2019
52. A.I. Gebi, *“Development and Characterization of Glass Ceramics from Coca-Cola Glass Bottle and Magnesite* (” Ahmadu Bello University, Zaria Nigeria, 2015)

Figures

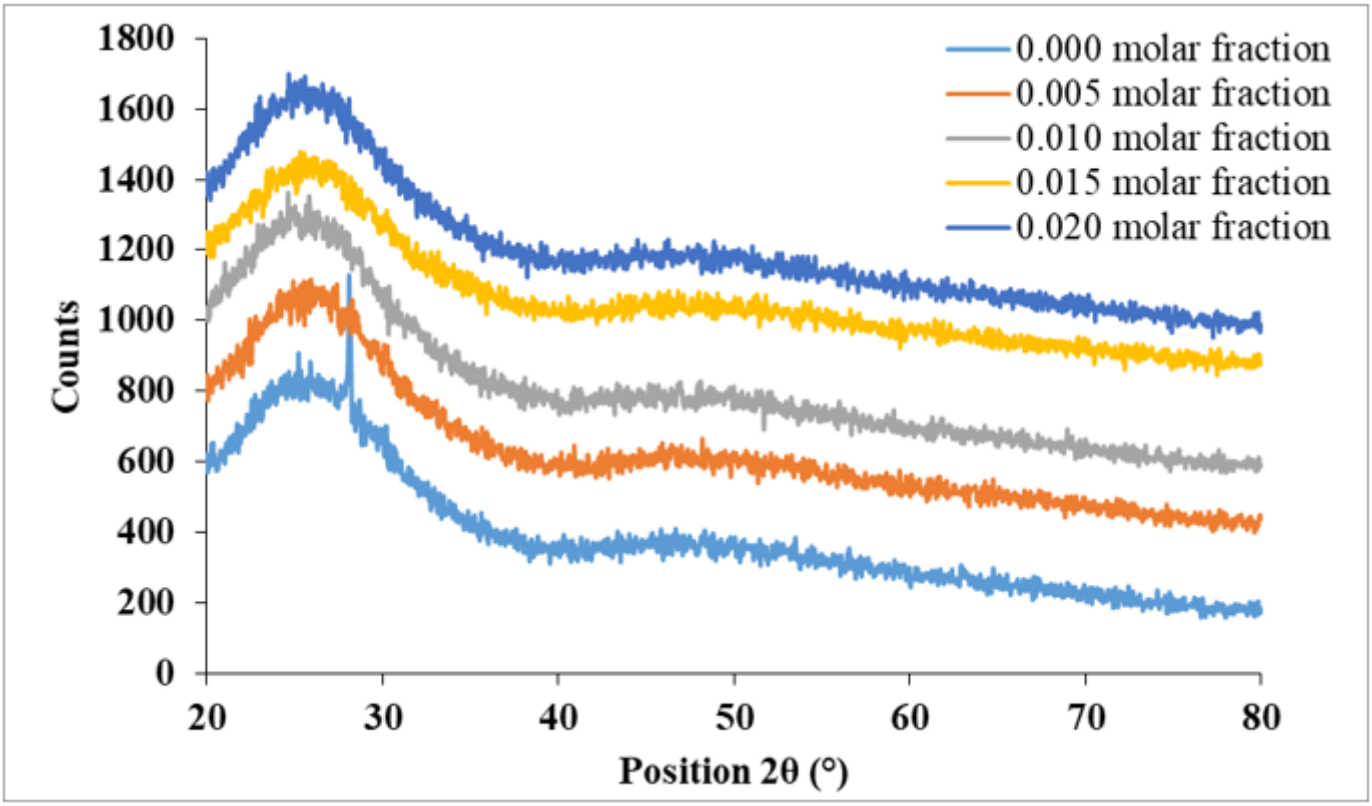

Figure 1

XRD Pattern for TeO_2 - B_2O_3 Doped CuO Glasses

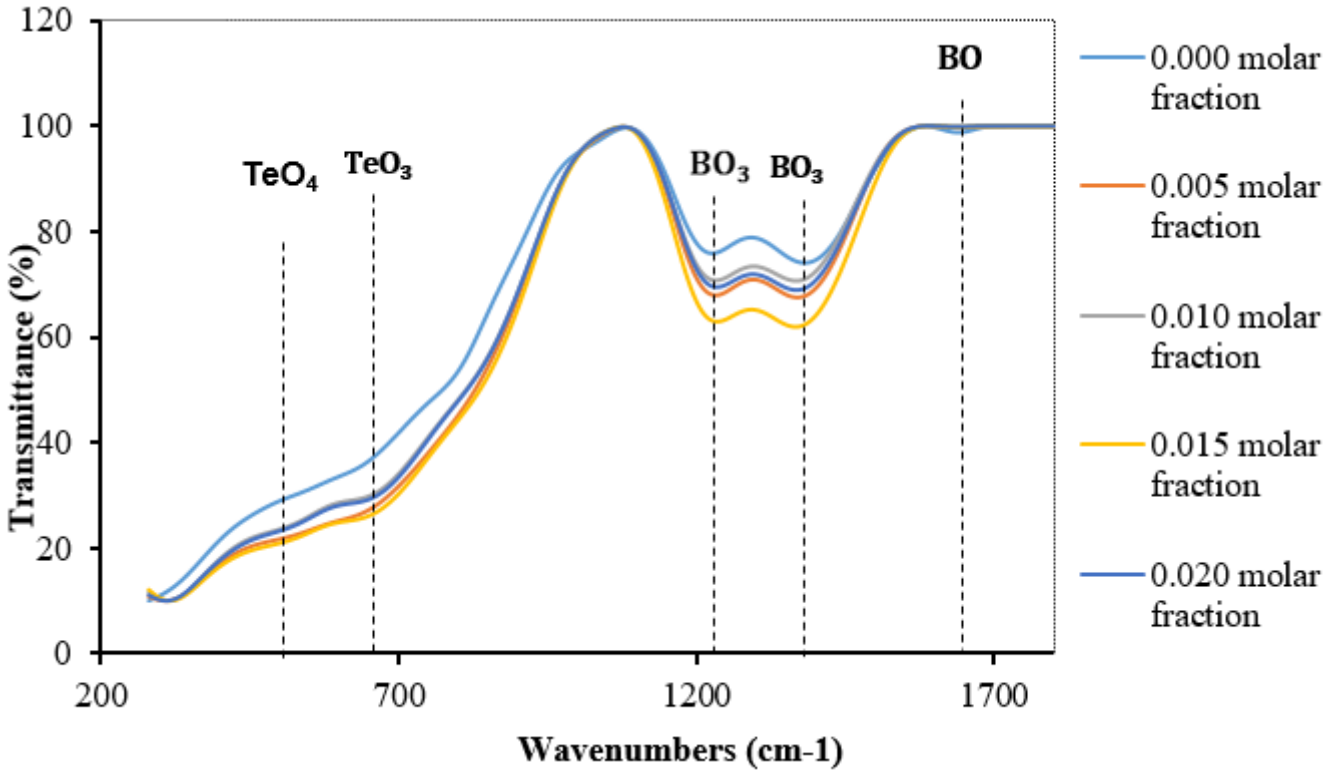

Figure 2

FTIR Spectra of Borotellurite Glasses Doped with Copper oxide

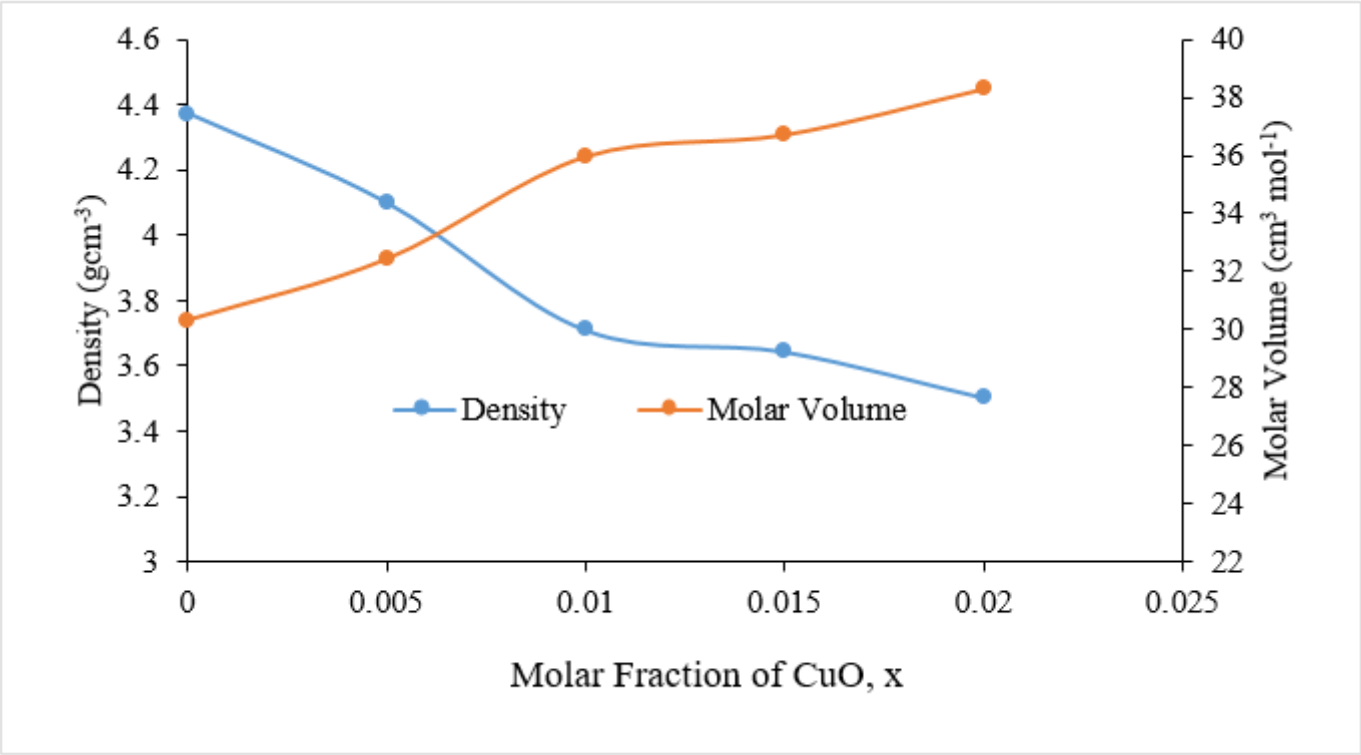

Figure 3

Density of Borotellurite Glasses Doped with various concentration of Copper Oxide

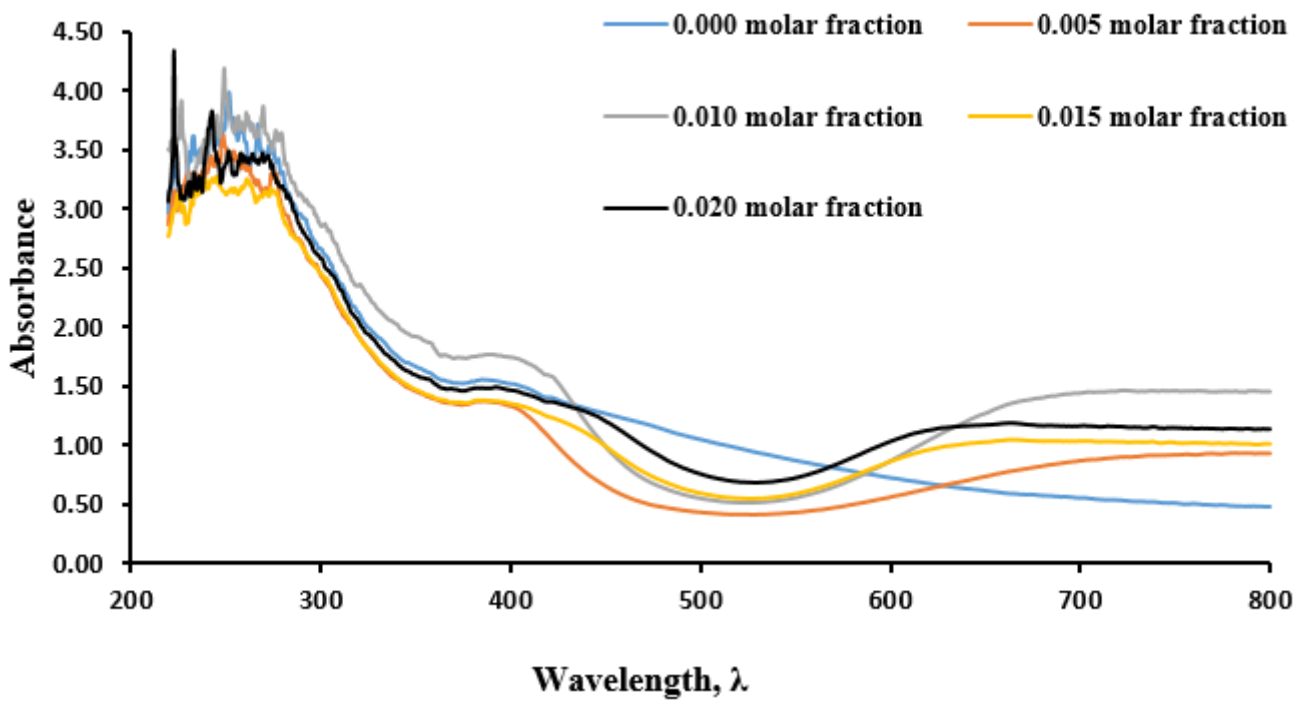

Figure 4

Optical Absorbance Spectra for various concentration of Copper Oxide Doped Borotellurite Glass System

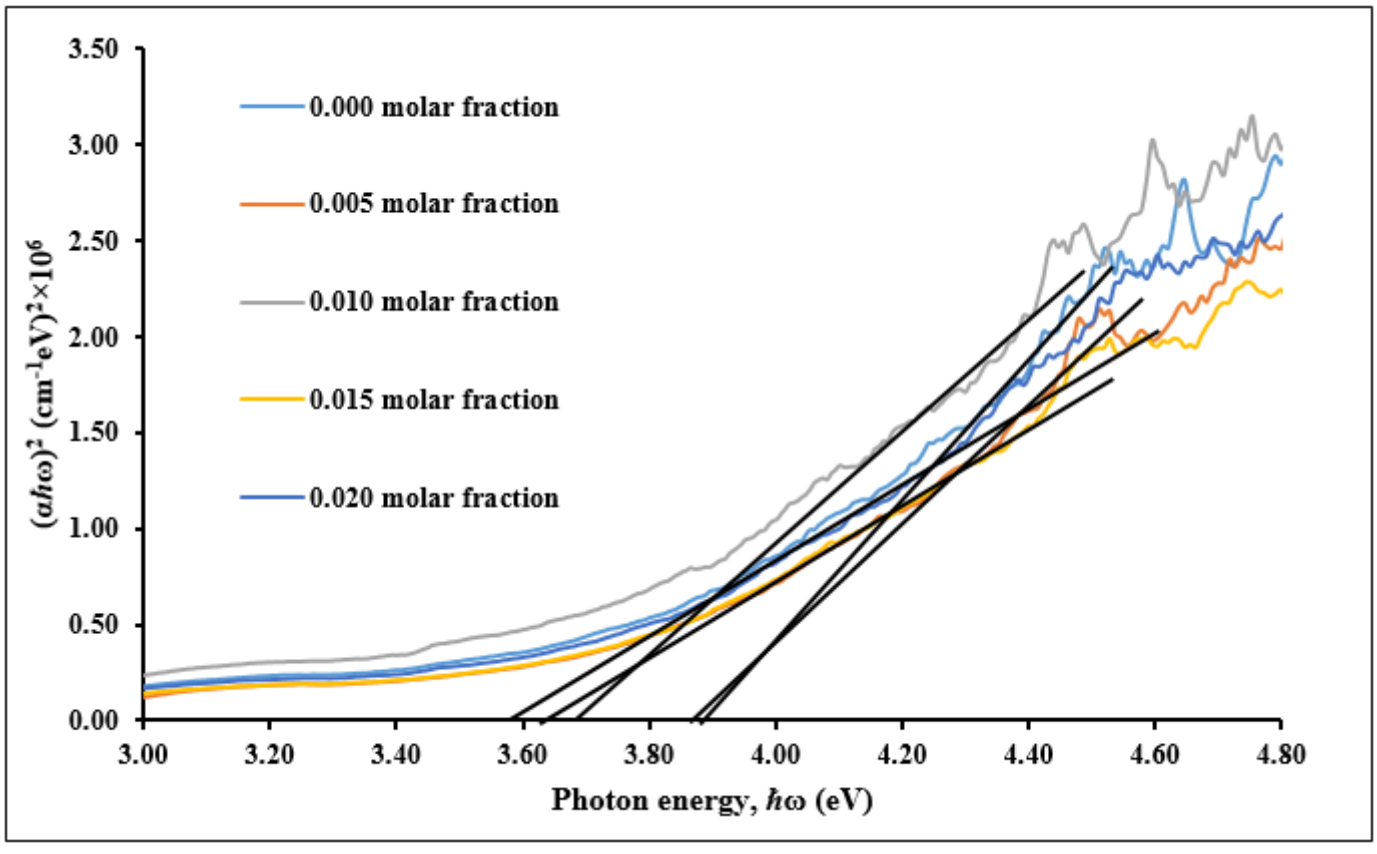

Figure 5

Graph of Borotellurite Glasses Doped with Various Concentration of Copper Oxide in respect to its Direct Energy Band Gap

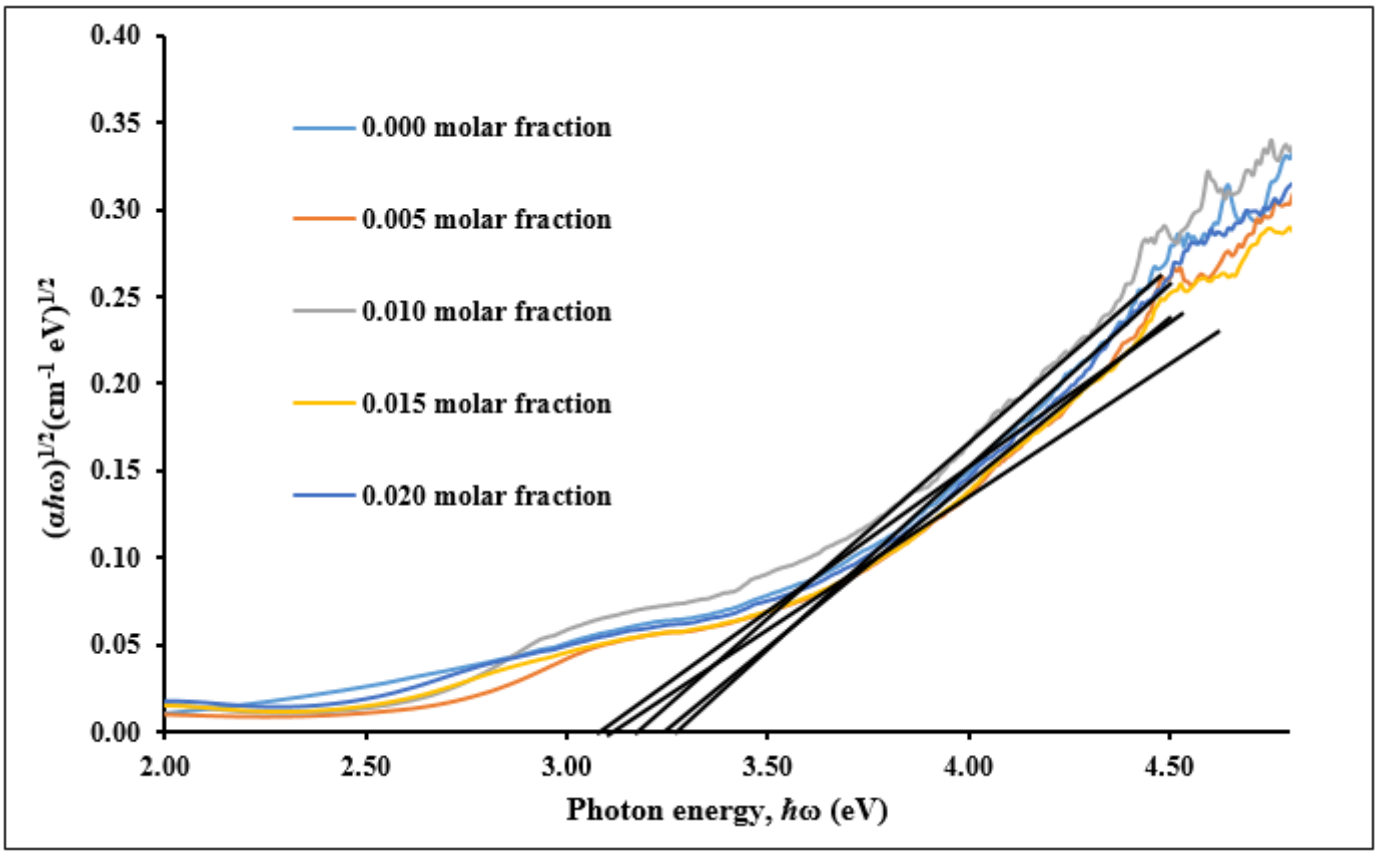

Figure 6

Graph of Borotellurite Glasses Doped with Various Concentration of Copper Oxide in respect to Indirect Energy Band Gap

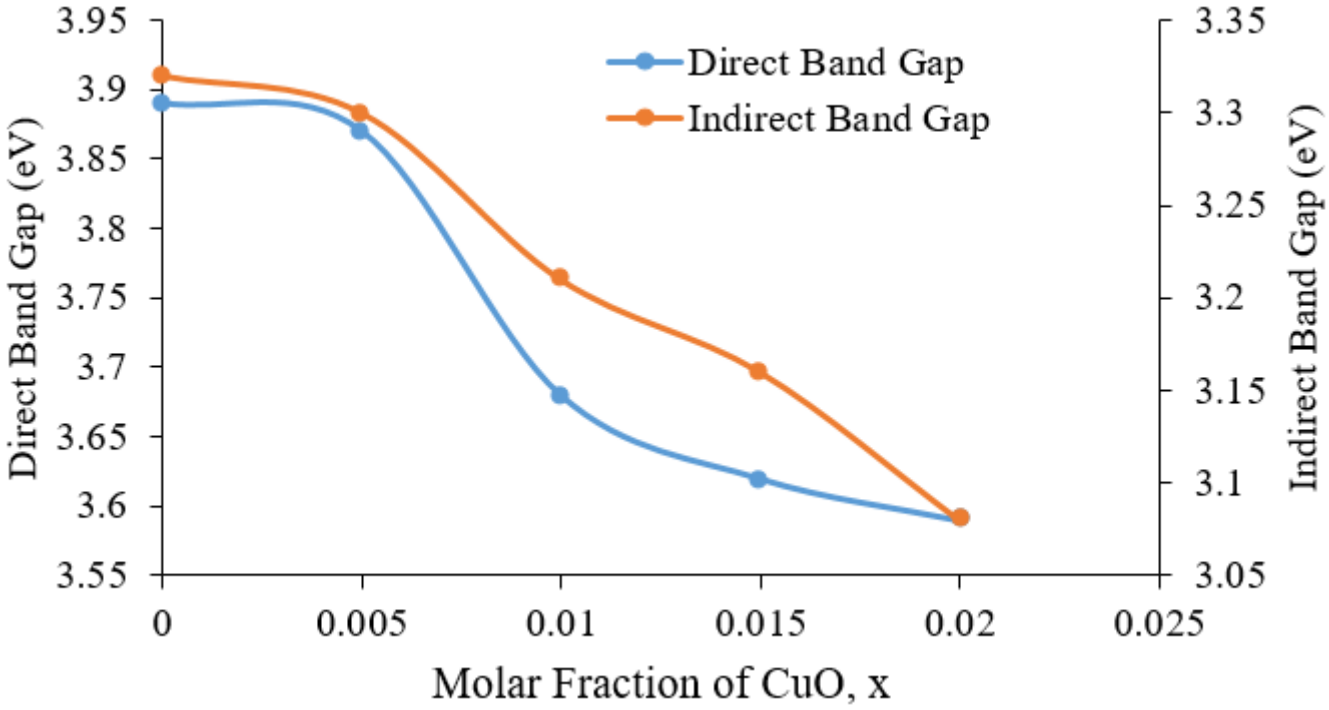

Figure 7

Graph of Direct and Indirect Energy Band Gaps for Borotellurite Glasses Doped with Various Concentration of Copper Oxide

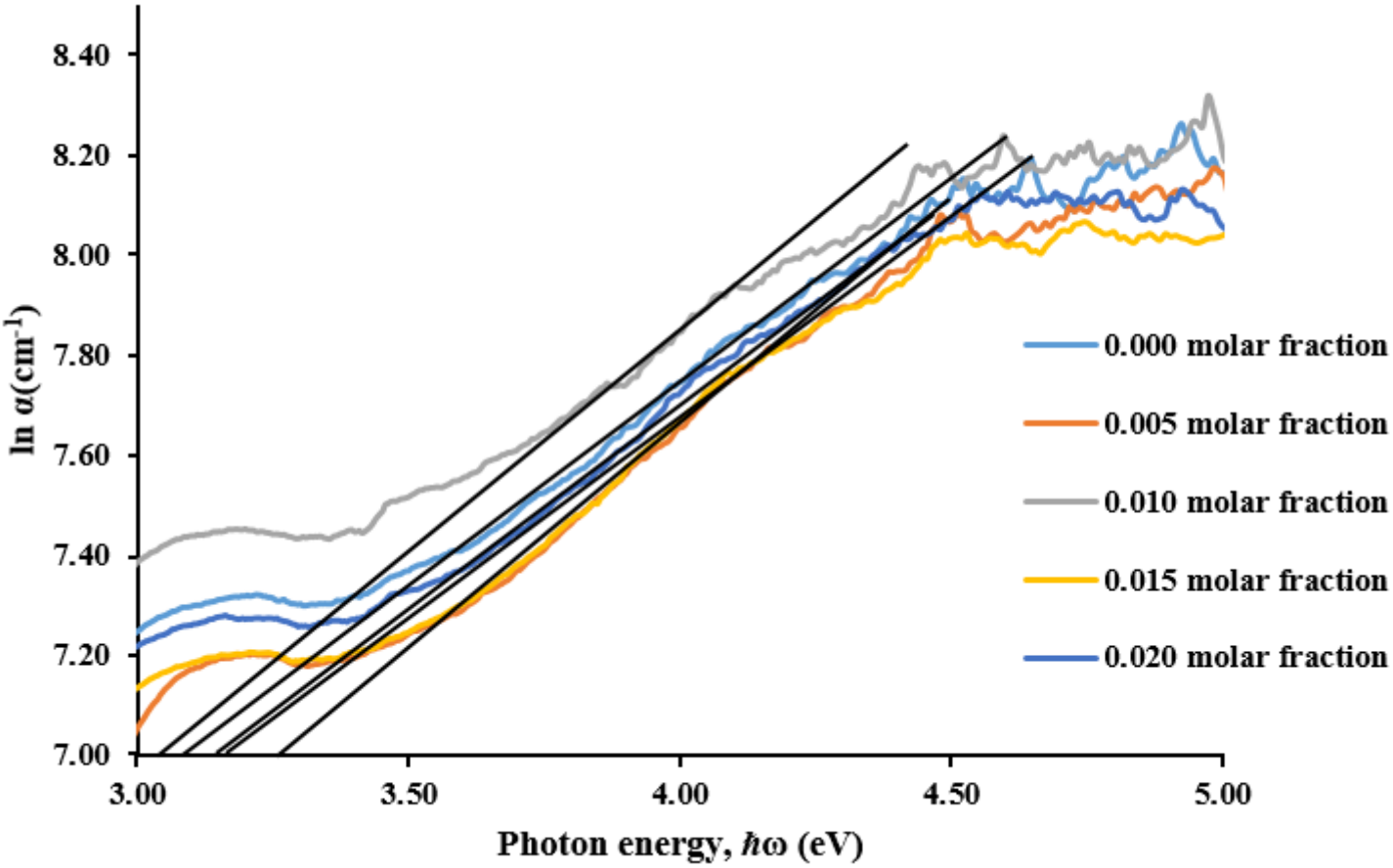

Figure 8

Absorption Coefficient (Optical), ln α against Photon Energy, ħω for Borotellurite Glasses Doped with Various Concentrations of Copper Oxide

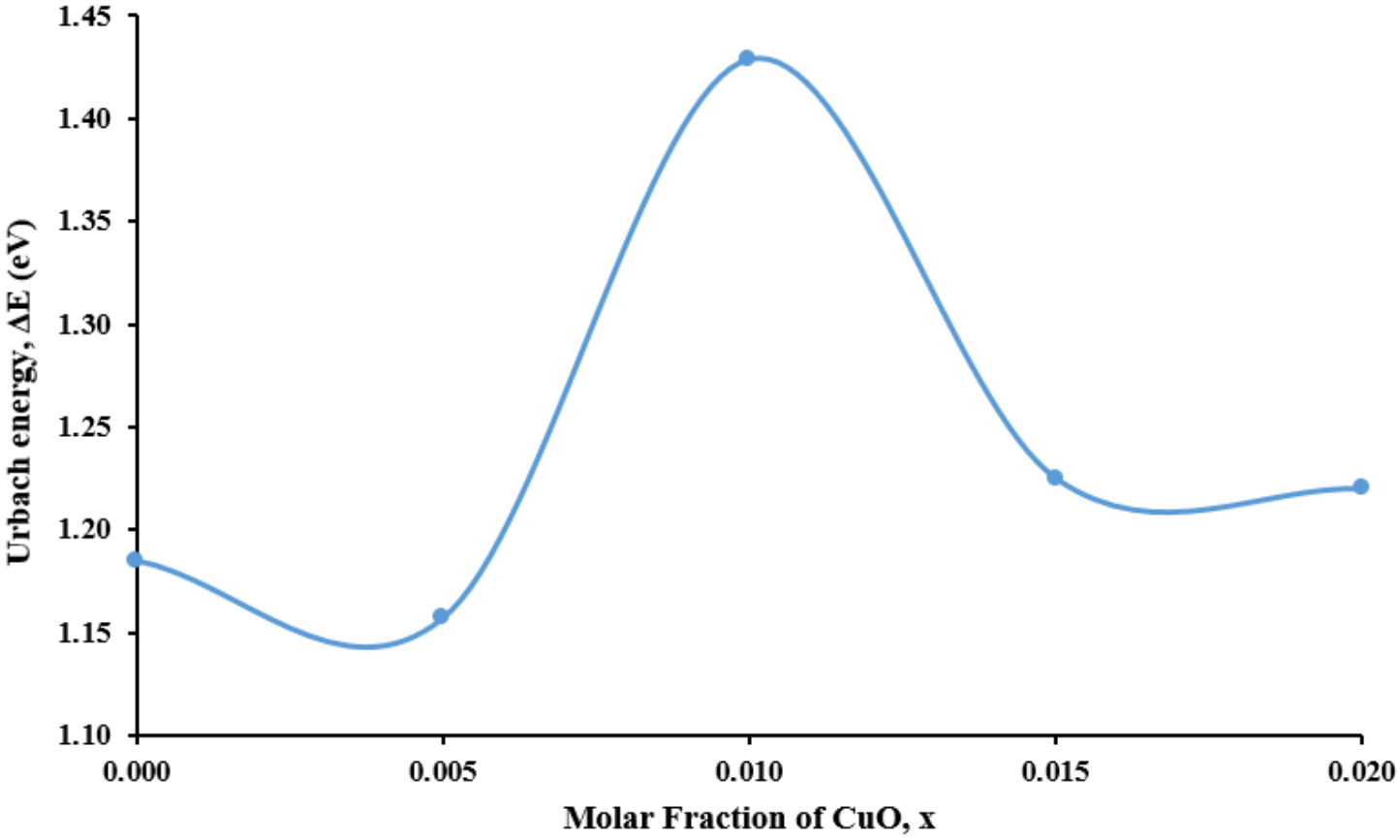

Figure 9

Urbach Energy, ΔE against Molar Fraction of CuO, x for Borotellurite Glasses Doped with Various Concentration of Copper Oxide

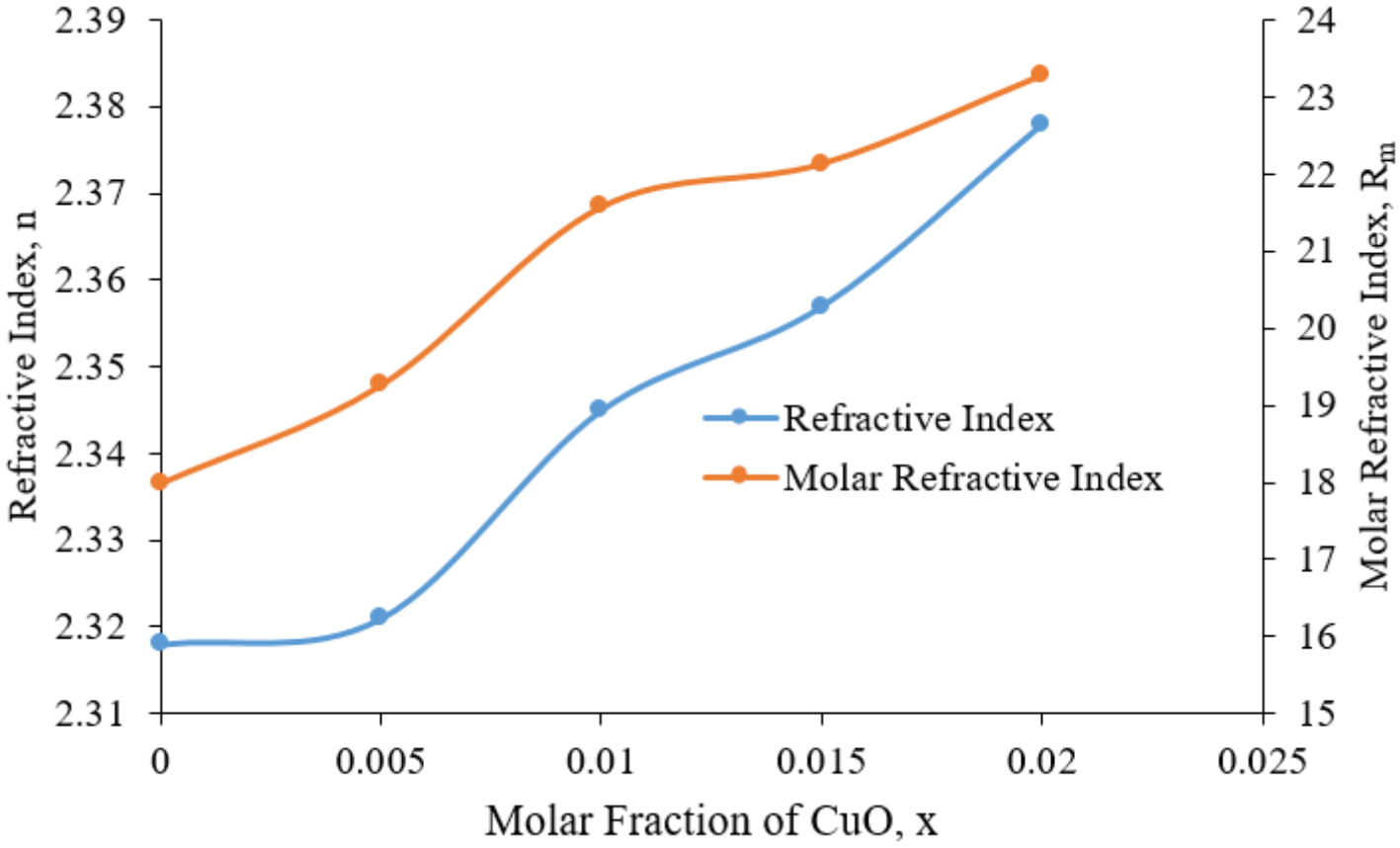

Figure 10

Refractive Index and Molar Refractive Index of Borotellurite Glasses Doped with Various Copper Oxide Concentration

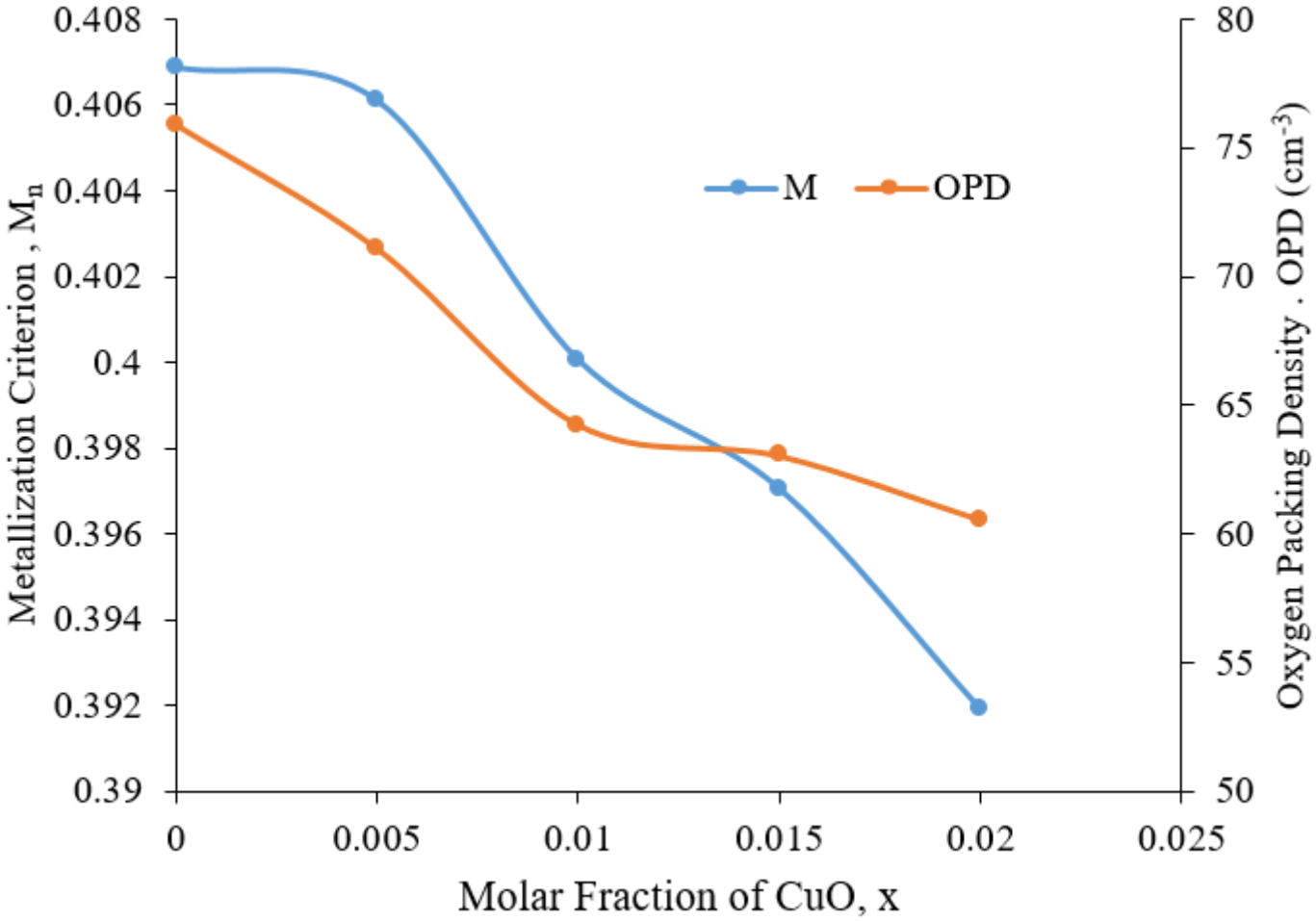

Figure 11

Refractive Index Based Metallization Criterion and Oxygen Packing Density of Borotellurite Glasses Doped with Various Concentration of Copper Oxide

Figure 12

Coefficient of Transmission and Reflection Loss against the Molar Fraction of CuO in Borotellurite Glasses Doped with Various Concentration of Copper Oxide

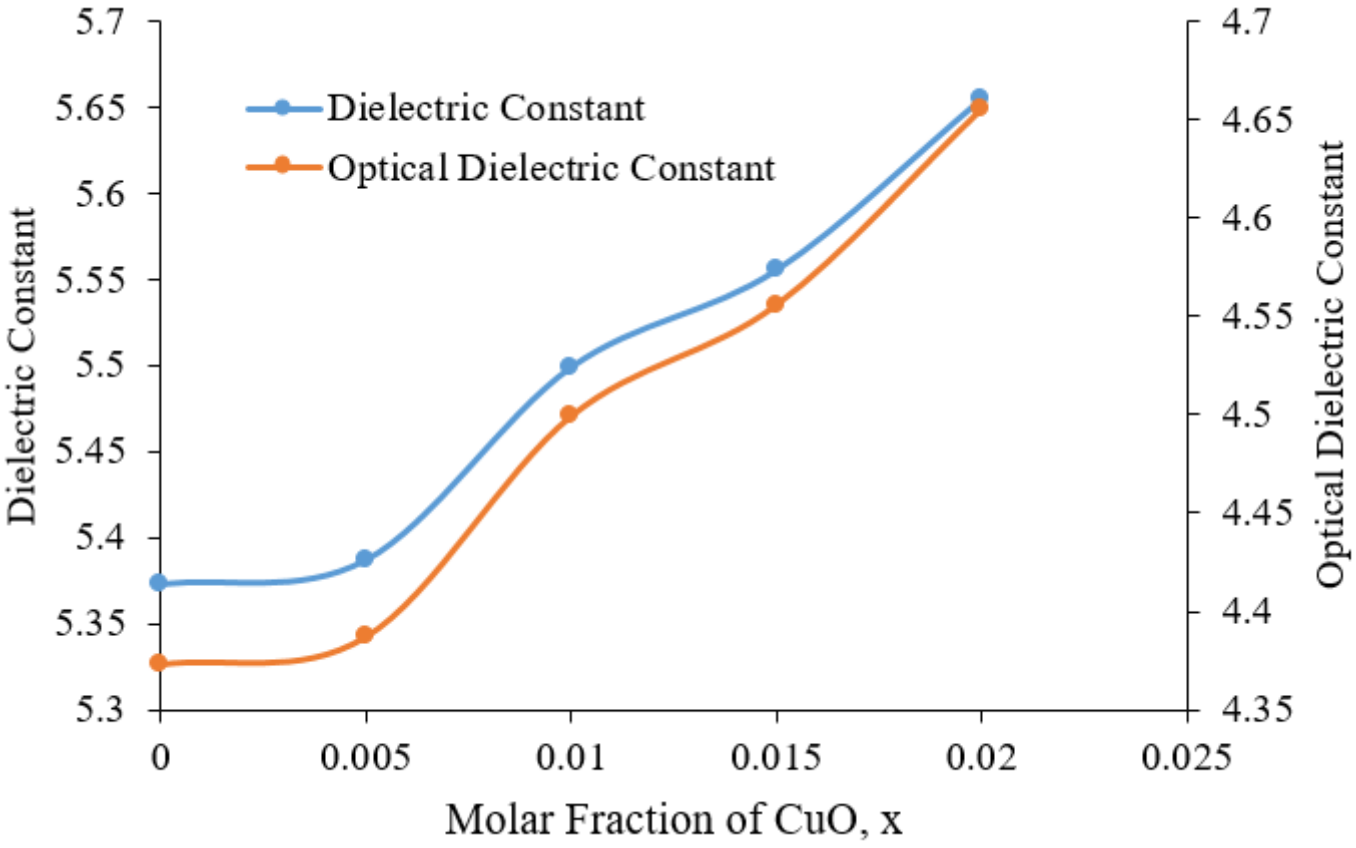

Figure 13

Dielectric Constant and Optical Dielectric Constant of Borotellurite Glasses Doped with Various Concentration of Copper Oxide